

# Measuring uncertainty in DOA-based signal localization

Christopher Patton

June 1, 2015

## Abstract

The QRAAT ("Quail Ridge Automated Animal Tracking") system provides ecologists and animal biologists with high resolution animal tracking data. It is comprised of a network of radio receivers deployed across the Quail Ridge Reserve in Napa County, California, and uses radio telemetry to simultaneously track a variety of animals including small field mice, birds, and foxes. QRAAT improves the state of the art of small species tracking by automating the process, allowing the collection of movement data at any time scale while separating the researcher from the study environment. This article presents our direction-of-arrival mode of signal source estimation and provides a statistical treatment of location estimate uncertainty. We evaluate via simulation the performance of our measurements, as well as the QRAAT system over all. Our results reveal a method of measuring uncertainty that works well under a variety of conditions captured in our model.

## 1 Introduction

Tracking animal movement is a critical component of ecological and animal behavior research. It allows researchers to quantify a number of parameters, including home range, migration patterns at various time scales, and survival rates, giving insight into a species' hunting, foraging, and social patterns. GPS technology provides a reliable means of gathering movement data; however, the bulky GPS units remain unsuitable for small species such as mice and birds. Alternatively, it is possible to fabricate a simple, low-power radio transmitter weighing only a few grams that allows a tagged animal to move about unencumbered; the target can be tracked with a commodity radio receiver and directional antenna.

Radio technology has led to numerous studies of a wide variety of species, as well as a number of methodologies for carrying them out. In their seminal work *Analysis of Wildlife Radio-Tracking Data* [1], Gary White and Robert Garrott address a number of issues central to designing and implementing such studies: What affect does tagging the animal have on observed behavior? How many members of the target population should be tagged? How frequently should the positions of the transmitters be measured? How are measurements made and how does one quantify error of these measurements? What is an acceptable level of estimate error? The answers to these questions invariably depend on the hypothesis in question. For example, a home range study might require a large sample of the population to be tagged, but observations can be made less frequently. On the other hand, a correlation study (e.g. mating practices) might require a large number of samples of just a few targets. It is critical in any case to obtain reliable estimates of the transmitters' location. Furthermore, there is always some uncertainty associated with these measurements, since radio telemetry is inherently noisy. Understanding the factors that induce error on estimates and quantifying this error is the subject of the current work.

Researchers have traditionally relied on hand-tracking techniques [1]. These approaches involve capturing a representative sample of the target population and tagging them with small, low-power radio transmitters, each identified by a unique transmission frequency. These devices typically transmit a fixed-length, periodic pulse that is audibly distinguishable from background radio traffic; alternatively, the signal can be modulated with sensor data such as heart or respiration rate of the individual. The transmitter can be localized by triangulating its position with two known bearings from fixed observation points. A researcher

stands in some location near the study area and listens for the transmitter's signal with a directional antenna. She finds the direction in which the signal is the strongest and records a compass bearing and her own location. This defines a ray in two dimensions from a fixed position with bearing to the transmitter. Another researcher does the same from a different location; assuming both have line of sight to the transmitter, the point at which these rays intersect corresponds (ideally) to the transmitter's location.

This basic hand-held method remains the predominant mode of tracking of small species, but it has a number of deficiencies. First, it is labor intensive, requiring at least two researchers to take periodic measurements of the target's bearing. This can become difficult or infeasible if the target travels over a large area, the study requires frequent samples, or if there are many targets to track. Second, human presence in the study area will likely influence the behavior of the animals being studied; it is therefore prudent to distance oneself as far as possible from the study area, but this induces error on the position estimates. Third, the manual bearing measurements are highly subjective in nature. Since the researcher chooses the bearing based on what direction the signal is the loudest, it is possible that two people choose different bearings in the same experiment. The distributions of their estimates may differ as a result, making it challenging to meaningfully quantify the precision of a position estimate at all. This fact coupled with the lack of standardization of such techniques makes it difficult to compare different studies and datasets.

The QRAAT system addresses these issues by automating the process. The need for automation is two-fold: one, traditional hand-tracking does not scale to large or complex studies; two, automation guarantees that measurements are made in a uniform manner, allowing the researcher to usefully quantify error of estimates. The system employs a number of fixed radio receivers over a study area that record the transmitters' signals, estimate their bearings, and send this information to a central server to be processed into position estimates. Each receiver is comprised of a specialized antenna and radio unit called a Rapid Multichannel Goniometer (RMG) designed specifically to discriminate the signal's bearing [6]. The signal is digitized and analyzed by a software-defined radio, necessitating a computer at each site for processing and storing the signal. Each node in our system is equipped with solar power and a wireless network for facilitating communication and transmission to a central server. Our system enables the collection of high resolution movement data without disturbing the study area beyond the installation of receivers and trapping and tagging targets.

The current work focuses on the problem of position estimation from recorded signals and on measuring the uncertainty of these estimates. In section 2 we briefly introduce the problem of localization in general and elaborate the basic approaches to solving it. We will also review traditional hand-tracking and how uncertainty is measured in that setting. We then present our methodology in detail in section 3. Our method of position estimation is based on a mathematical model of the transmitter's signal as recorded by an array of antennas with which it is possible to discriminate the signal's most likely *direction-of-arrival* (DOA) by comparing the recording with a database of pre-recorded signals from known bearings. We devise a method for estimating the signal's source using the DOA from two or more receiver sites and derive the estimate's covariance and confidence intervals. Finally, section 4 evaluates the performance of our position and covariance estimates. We simulate our model under various conditions which impact the distribution of estimates and examine the performance of the QRAAT deployment at Quail Ridge as a whole.

## 2 Background

There are two ways to compute the position of a transmitter given information from multiple observation points. Suppose we do not know where the transmitter is, but we know exactly how far away it is from a receiver. In the two-dimensional case, this defines a circle of possible positions encompassing the receiver; if we add a second site, the two circles will intersect at one or two possible points; add a third and the circle will intersect at precisely one point. (See figure 1a for an illustration.) Let  $(a, b)$ ,  $(c, d)$ , and  $(e, f)$  be known positions of receivers and  $X$ ,  $Y$ , and  $Z$  be corresponding distances to the transmitter. *Trilateration* is a

process of solving the system of equations

$$\begin{aligned}(x - a)^2 + (y - b)^2 &= X^2 \\ (x - c)^2 + (y - d)^2 &= Y^2 \\ (x - e)^2 + (y - f)^2 &= Z^2\end{aligned}\tag{1}$$

with respect to  $x$  and  $y$ . Error is introduced into this method when the distances from the sites to the receiver are not precisely known, in which case the system may not have a solution. This may be addressed in practice by assuming a distribution of the noise on the measurement of distance and finding the solution that maximizes the *likelihood* of the observations  $X$ ,  $Y$ , and  $Z$ . Just how the noise should be modeled depends on how the measurement is made; we discuss three major approaches in section 2.1.

Suppose alternatively that we know the bearing to the ~~the~~ transmitter from the receivers and not the distance. *Triangulation* is the process of finding the point at which bearings from two sites intersect. Referring to figure 1b, let  $\beta_1$  be the bearing (in radians) from  $(a, b)$  to the transmitter and  $\beta_2$  from  $(c, d)$ . The position of the transmitter is given by finding  $x$  and  $y$  such that

$$\frac{x - a}{\cos \beta_1} = \frac{y - b}{\sin \beta_1} \text{ and } \frac{x - c}{\cos \beta_2} = \frac{y - d}{\sin \beta_2}.\tag{2}$$

When the bearings are not precisely known there will be a solution, but it will not correspond precisely to the transmitter's true position. Moreover, if we add a third receiver, the system of equations will likely not have a solution at all. Just as in trilateration, we can model the distribution of noise induced on our observations  $\beta_1, \beta_2, \dots$  and find the most likely position  $(x, y)$  with respect to the model. We discuss triangulation-based approaches and motivate our own methodology in section 2.2.

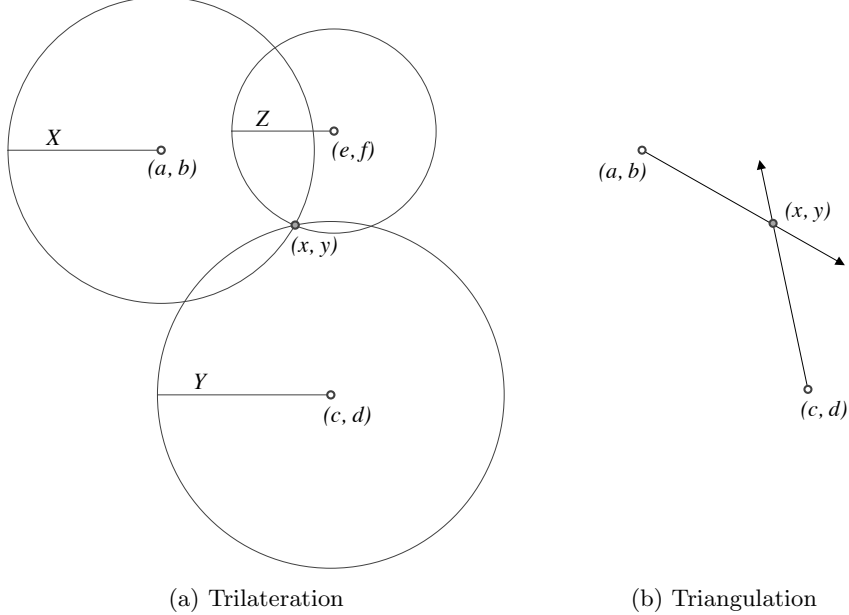


Figure 1: Trilateration versus triangulation. Compute a transmitter's position  $(x, y)$  from known distances from at least three sites or known bearings from at least two sites.

## 2.1 TOA, TDOA, and RSS

The simplest trilateration technique is the *time-of-arrival* (TOA) method. Since the speed of light is constant, there is a linear relationship between the distance a signal travels from transmitter to receiver and the time required to traverse that distance. Suppose it is known that the transmitter sends a signal every 5 seconds.

Knowing precisely when the transmitter began transmitting, the receiver subtracts the time the signal was sent from the time it was recorded; multiplying by the speed of light yields the distance traveled. Accuracy and precision are lost due to system noise in recording the time of arrival. First, even in a dedicated circuit, there will be a certain amount of latency between arrival and the time recording, varying as a result of temperature and other factors. Second, background noise on the transmission frequency affects the triggering mechanism itself. These conditions may be modeled in the experiment as a Gaussian random variable with zero mean [4, 13] such that the traversal time is  $t = t_{(x,y)} + n$ , where  $t_{(x,y)}$  is the distance between  $(x, y)$  and the receiver multiplied by the speed of light, and  $n \sim \mathcal{N}(0, \sigma^2)$ . Assuming that the observations from the receivers are independent (that is, the additive values are independent), we can easily express the joint probability density function (PDF) of our observations given  $(x, y)$ . From this we can derive the *maximum likelihood estimator* (MLE) for the signal's source with respect to our model by simply taking the natural log of the PDF. The value  $(\hat{x}, \hat{y})$  that maximizes this function is called the maximum likelihood estimate.

There are two requirements of TOA that hinder the deployment of such a system, particularly in the case of QRAAT. One, the receivers must know when the signal was transmitted, implying that the transmitter must modulate a timestamp into the signal. This incurs a cost in the complexity of the transmitter circuit, thereby requiring a larger battery and making the unit unsuitable for smaller animals. The *time-difference-of-arrival* (TDOA) method removes this constraint by modeling the pairwise difference of arrival times among the receiver sites [13]. Suppose there are  $k$  sites with arrival times  $t_1 \dots t_k$  and let  $t_0$  be the unknown send time. Let  $t_{i,j} = (t_i - t_0) - (t_j - t_0) = t_i - t_j$ , the difference of traversal times to distinct sites  $i$  and  $j$ . The TDOA of  $i$  and  $j$  is modeled as  $t = t_{i,j} + n$  where  $n$  is normally distributed with zero mean and  $t_{i,j}$  is a function of distance to  $(x, y)$ . The MLE of this model can be constructed similarly to TOA.

The second constraint on both TOA and TDOA systems is that the clocks of the receiver sites must be synchronized precisely in order to perform position estimation. Computer clocks are prone to drifting so it is necessary to facilitate communication between them, yet this may be infeasible for a variety of reasons. An alternative to these timing-based methods is to use *received-signal-strength* (RSS) in order to measure distance [4]. The signal strength of a transmitter is known to degrade as a function of distance; given the transmitter power at the signal source, we can estimate the distance traveled by the received signal strength. The function used to model degradation depends on the environment in which the signal is traveling [13]. RSS-based approaches overcome the synchronization constraint and can handle any signal modulation, but we must model the propagation of the signal through space. The best model depends on the transmission environment.

## 2.2 DOA

We turn now to triangulation, historically the most important position estimation method in our domain. We prefer direction-of-arrival over the foregoing for a number of reasons: one, triangulation requires just two sites where trilateration requires three; two, it is crucial to place the minimal burden on the transmitter, since simpler circuits result in lighter tags; three, our system should be robust to power and network availability, and clock synchronization may be infeasible or impossible when network resources are limited. The main drawback of DOA compared to the trilateration methods is increased complexity of the receiver antenna. Known methods for discriminating the signal's bearing in far-field tracking systems like QRAAT require an array of antennas to be installed, whereas TOA, TDOA, and RSS systems require just one per site. This increases power consumption, but our experience suggests that solar power suffices, at least at our site in northern California, for operating the receivers.

Similarly to the trilateration methods, the simplest approach is to model the noise induced on bearing measurements and derive the MLE. Suppose there are  $k$  observation sites and let  $(x_i, y_i)$  be the position of the  $i$ -th site. For the remainder of this paper, let

$$\beta_i(x, y) = \arctan\left(\frac{y - y_i}{x - x_i}\right) \quad (3)$$

denote bearing from site  $i$  to position  $(x, y)$ . We assume that the observed bearing is  $\theta_i = \beta_i(x, y) + n$  where  $n \sim \mathcal{N}(0, \sigma_i^2)$  for some  $\sigma_i^2$ . Let  $\mathbf{b} = [\beta_1(x, y) \dots \beta_k(x, y)]^T$  and  $\mathbf{r} = [\theta_1 \dots \theta_k]^T$ . Assuming the noise

distributions are independent between sites, we obtain the following probability density function of  $\mathbf{r}$  with respect to  $(x, y)$  [13]:

$$f(\mathbf{r}|x, y) = \frac{1}{\sqrt{(2\pi)^k \det \mathbf{C}}} \exp\left(-\frac{1}{2}(\mathbf{r} - \mathbf{b})^T \mathbf{C}^{-1}(\mathbf{r} - \mathbf{b})\right) \quad (4)$$

where  $\mathbf{C}$  is a diagonal matrix with  $\sigma_1^2 \dots \sigma_k^2$  along the diagonal. An algorithm that maximizes  $f(\mathbf{r}|x, y)$  over all choices of  $x$  and  $y$  is a maximum likelihood estimator of this model.

The basic deficiency of this method is that we must assume a variance on bearings. This can be overcome, at least partially, by measuring it. Suppose the position of the transmitter is known, or alternatively the position is not known, but it is known that the transmitter is stationary. Measure the bearing a number of times from each site and create a histogram of the observations; assuming normality, the variance can be estimated from this empirical distribution. An issue that arises, especially when these measurements are made by hand, is independence of each of these trials [1, §5]. However, a more fundamental problem is that the variances are subject to change over time as the target moves about. In particular, one would suspect intuitively that variance of bearing would increase as the target moves away from the observation site, since the signal may be indistinguishable from the background noise at a distance. We refer to the received signal strength relative to the background noise as the *signal-to-noise-ratio* (SNR).

The approach of modern, automated direction-of-arrival systems (including QRAAT) is to model the error induced on the received signal itself. This error can be measured directly; when the receiver records a signal, it also records a sample of the background noise on the transmission frequency just before the signal arrived. The variance of bearing can then be estimated from the known signal-to-noise. We present the signal model employed in QRAAT in section 3.1 and consider its extension to position estimation in section 3.3.

### 2.2.1 Quantifying error

An essential feature of any signal source localization methodology is to provide a measurement of uncertainty associated with position estimates so that users have a sense of what sort of inferences can be made from the data. To this end it is crucial to define precisely what is meant by uncertainty. We think of the ML estimate  $(\hat{x}, \hat{y})$  as a random variable whose distribution depends on the signal model. The *covariance* of the estimate is a  $2 \times 2$  matrix indicating the variance of  $\hat{x}$  and  $\hat{y}$  (diagonal values) and how these vary together (off-diagonal values). If the two dimensions are independent, then the off-diagonal values will be zero. Following [12], we construct a *confidence region* from the covariance defined by a closed interval of the plane encompassing the estimated position with the following property: fix the position of the transmitter and suppose we estimate the position and covariance a number of times, and for each covariance matrix we compute a 95%-confidence region. At least 95% of the time, the true parameter  $(x, y)$  will fall within the confidence region of the estimate. The derivation of covariances and confidence regions for our estimates is the subject of section 3.4. Note that the prescribed property only holds under certain conditions; this point is addressed in section 4. In that section we will also elaborate the factors that influence the distribution of estimate, including noise, sample size, and systematic factors such as distance to the receivers and angle of intersection of bearings.

### 2.2.2 Historical approaches

For completeness, we indicate the methodologies historically significant to the animal tracking community. In classic hand-tracking, the estimate of position is obtained from two bearings by solving for  $x$  and  $y$  in equation 2. White and Garrot describe a rudimentary method for measuring the uncertainty of an estimate obtained in this way [1]. Suppose the standard deviation of both observation points are known (or measured). Assuming the bearings are normally distributed, the 95%-confidence intervals for the bearings are  $\hat{\theta}_1 \pm 1.96\sigma_1$  and  $\hat{\theta}_2 \pm 1.96\sigma_2$ . In two dimensions, these define wedges extending from the observation points towards the target; the so called *error polygon* is the region where these wedges intersect.

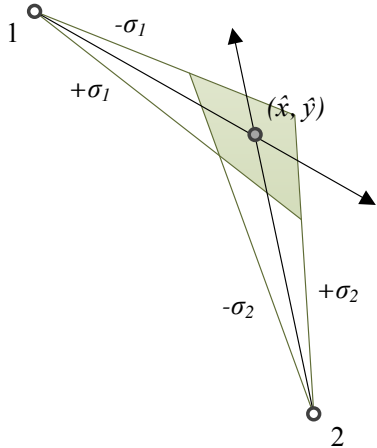


Figure 2: An error polygon.

This technique intuitively captures a number of factors that cause error in the position estimate. The salient features of the error polygon are area and elongation. As the distance between sites and the transmitter increases, so do the widths of the wedges and thereby the area of the polygon. On the other hand, as the angle of intersection between the bearings approaches  $180^\circ$ , the polygon becomes elongated. While this measurement may be useful as a qualitative tool, it is not clear how to make it statistically rigorous and draw inferences about the estimate or its distribution.

As far as we are aware, Russel Lenth [2] was the first to derive a maximum likelihood estimator for position. Observed bearings are assumed to be independent and follow the von Mises distribution, which resembles the angular Gaussian distribution in that it has one symmetric lobe, but has a simpler analytic form. The distribution has three parameters: the observed bearing  $\theta_i$ , the true bearing  $\mu_i$ , and a concentration parameter  $\kappa$  analogous to variance. The MLE is a non-convex system of equations with a simple form, making it suitable for

running on the computers of the time (1981). The estimator does not depend on  $\kappa$ , so the ML estimate of the model can be obtained without measuring variance. Lenth also indicates how to derive the covariance (which does depend on  $\kappa$ ) of estimates, as well as a variety of M-estimation techniques for robust estimation in complex signal environments. These are evaluated by White and Garrott and the results are summarized in [1, §4]. Other extensions to the basic model are considered, the most important of which, for our purposes, is handling multi-directional antenna arrays in which the bearing estimate is one of two or more bearings that differ depending on the antenna configuration. The MLE is constructed by generalizing the von Mises distribution so that it has many lobes. Such a generalization as well as a method for obtaining distribution parameters based on observed bearings is considered in [5].

The focus of animal tracking methodology has shifted in recent years to movement modeling, in which physical or behavioral assumptions of the target are used to filter and/or smooth position estimates in time. An early method was devised by Richard Anderson-Sprecher and Russel Lenth that fits a spline to an animal track in time based on direction-of-arrival data from multiple receivers [3]. Today, the most conventional method is the Kalman filter [16], which uses inertial characteristics of the target to smooth time-sequenced GPS data. This approach is best suited for fast moving targets where the magnitude of error is less than the speed at which the target travels, but there are other methods potentially useful for a wider variety of subjects [17, 18].

### 3 Position estimation

Our method of tracking builds upon the masters thesis of Todd Borrowman [6], which describes the construction of an antenna array and software defined radio for receiving and recording signals from a number target transmitters simultaneously. Borrowman outlines a probabilistic model for signal direction-of-arrival estimation based on the antenna pattern. This section presents the results of that work and describes how the direction finder can be used, in conjunction with multiple receiver sites, to estimate the position of a transmitter. For the purpose of understanding this work concretely, one may think of the transmitter generating a fixed-length, periodic pulse.<sup>1</sup> Thus, when we speak of the signal, we mean a recording of this pulse as well as sample of the background noise on the same frequency. In fact, all of the methods presented in this paper are independent of the transmitter's modulation.

Section 3.1 outlines the signal model and deals with some practical and theoretical implications of our assumptions. Section 3.2 briefly presents various direction finding methods and how they can be applied to

<sup>1</sup> For example, a common transmitter make has a pulse width of 20 milliseconds and period of about 2.3 seconds. Since the transmitter is composed of a minimal power circuit, the actual period fluctuates as a result of environmental conditions and battery load.

our system. Section 3.3 describes our numerical method of position estimation using a generic direction finder and section 3.4 provides a statistical treatment of our estimates' covariance. Finally, we present simulation results in section 4 that justify our assumptions.

### 3.1 Signal model

In what follows we think of a bearing from a receiver as an element of  $[0, 2\pi)$  where 0 radians indicates east. We consider a model for the direction of arrival of a signal to an antenna array with  $m$  channels<sup>2</sup> building upon [7, 8]. Let  $\mathbf{v} \in \mathbb{C}^m$  represent the eigenvalue decomposition of the recorded signal. We assume that

$$\mathbf{v} = T\mathbf{g}(\theta) + \mathbf{n} \quad (5)$$

where  $\mathbf{g}(\theta) \in \mathbb{C}^m$  corresponds to the normalized antenna pattern ( $|\mathbf{g}(\theta)| = 1$  for all  $\theta$ ) with respect to the direction of arrival  $\theta$ . Called the *steering vector* of the receiver with respect to  $\theta$ , one may think of  $\mathbf{g}(\theta)$  as the signal we "expect" to see when the source of the signal has this bearing to the receiver. The steering vectors are generated by recording signals from known bearings to the receiver in a process called *calibration*, discussed briefly in section 3.1.1.  $T$  is the *transmission coefficient* of the signal, modeled as a circularly symmetric, complex Gaussian scalar with zero mean: that is,  $T \sim \mathcal{N}(0, \sigma_T^2)$ . This value captures several characteristics of the experiment, such as the transmission power of the signal source, the distance to receiver, and other features that influence the magnitude of the signal's eigenvalue decomposition. Lastly,  $\mathbf{n} \in \mathbb{C}^m$  represents the additive noise vector. In order to develop our model, we assume that the signal noise is uncorrelated between channels. In particular, we'll take the elements of  $\mathbf{n}$  (the *channel noise*) to be independently and identically distributed, circularly symmetric, complex Gaussian random variables with 0 mean; that is,  $\mathbf{n} \sim \mathcal{N}(0, \sigma_n^2 \mathbf{I})$ .

By assumption, the probability density function of  $\mathbf{v}$ , given a direction of arrival  $\theta$ , is

$$f(\mathbf{v}|\theta) = \frac{1}{\pi^n \det \mathbf{R}} \exp(-\mathbf{v}^H \mathbf{R}^{-1} \mathbf{v}) \quad (6)$$

where  $\mathbf{R} \in \mathbb{C}^{m \times m}$  is the covariance matrix of  $\mathbf{v}$ . To compute  $\mathbf{R}$ , observe that

$$\mathbf{E}[\mathbf{v}] = \mathbf{E}[T\mathbf{g}(\theta) + \mathbf{n}] = \mathbf{E}[T\mathbf{g}(\theta)] + \mathbf{E}[\mathbf{n}] = 0 + 0$$

since  $\mathbf{v}$  has zero mean if  $T$  is zero mean. (Similarly, the expected value of  $\mathbf{n}$  is zero.) Thus,

$$\begin{aligned} \mathbf{R} &= \mathbf{E}[(\mathbf{v} - \mathbf{E}[\mathbf{v}])(\mathbf{v} - \mathbf{E}[\mathbf{v}])^H] && \text{Def. of covariance.} \\ &= \mathbf{E}[\mathbf{v}\mathbf{v}^H] && \mathbf{E}[\mathbf{v}] = 0. \\ &= \mathbf{E}[(T\mathbf{g}(\theta) + \mathbf{n})(T\mathbf{g}(\theta) + \mathbf{n})^H] \\ &= \mathbf{E}[TT^H\mathbf{g}(\theta)\mathbf{g}(\theta)^H] + \mathbf{E}[\mathbf{n}\mathbf{n}^H] \\ &\quad + \mathbf{E}[T\mathbf{g}(\theta)\mathbf{n}^H] + \mathbf{E}[T^H\mathbf{g}(\theta)^H\mathbf{n}] \\ &= \mathbf{E}[TT^H]\mathbf{g}(\theta)\mathbf{g}(\theta)^H + \mathbf{E}[\mathbf{n}\mathbf{n}^H] + 0 + 0. \end{aligned}$$

We obtain the last line by observing that  $\mathbf{g}(\theta)$  is a deterministic function and assuming that  $T$  and  $\mathbf{n}$  are non-coherent [7]. We may rewrite the covariance matrix of  $\mathbf{v}$  in the following way:

$$\mathbf{R} = \sigma_T^2 \mathbf{g}(\theta)\mathbf{g}(\theta)^H + \sigma_n^2 \mathbf{I} \quad (7)$$

The quantity  $\sigma_T^2/\sigma_n^2$  is the signal-to-noise ratio of our model. Since  $\sigma_T^2$  and  $\sigma_n^2$  are not known, these are estimated from the recorded signal. For each recording, we sample the noise floor and estimate its covariance directly to obtain an  $m \times m$  matrix  $\Sigma$ , our estimate for the quantity  $\sigma_n^2 \mathbf{I}$ .  $\sigma_T^2$  is estimated as  $s^2 = \rho - \text{tr}(\Sigma)$  where  $\rho$  is the observed signal power. Based on the measurements of the signal and background noise, we obtain the following estimate of the signal's covariance matrix, given  $\theta$ :

$$\mathbf{R} \approx s^2 \mathbf{g}(\theta)\mathbf{g}(\theta)^H + \Sigma \quad (8)$$

---

<sup>2</sup> In our case,  $m = 4$ .

In what follows, we denote an observation derived from the recorded signal as the triple  $(\mathbf{v}, \rho, \Sigma)$ , where  $\mathbf{v} \in \mathbb{C}^m$  denotes the eigenvalue decomposition of the signal,  $\rho \in \mathbb{R}$  the signal power, and  $\Sigma \in \mathbb{C}^{m \times m}$  the covariance matrix of the channels' background noise.

### 3.1.1 Collecting the steering vectors

In order to determine the most likely direction-of-arrival for our observation, we compare  $\mathbf{v}$  to a finite set of previously recorded signals with known bearings. If the steering vector  $\mathbf{g}(\theta)$  is most “similar” to  $\mathbf{v}$  (with respect to  $\rho$  and  $\Sigma$ ) then  $\theta$  is our estimate of the bearing to the signal source. Suppose receiver  $i$  is located at  $(x_i, y_i)$ , and the transmitter, located at  $(x, y)$ , transmits a pulse recorded as  $(\mathbf{v}^*, \rho^*, \Sigma^*)$  at the receiver. If the observed signal to noise ratio of the signal is sufficiently high, then we normalize  $\mathbf{v}^*$  and take it as our steering vector  $\mathbf{g}(\beta_i(x, y))$ .

A receiver is *calibrated* by performing this experiment for as many bearings from the receiver as are feasible. For example, one might decide to record a steering vector for bearings corresponding to whole degrees, i.e.  $0^\circ, 1^\circ, 2^\circ, \dots, 359^\circ$ . It is critical that there is line of site to the receiver for the calibration to be valid; depending on topographical characteristics of the research area, this may not be possible. A least squares method for filling in gaps in the bearing spectrum with modeled steering vectors is presented in [7]; however, a more popular approach is to use the NEC (“numerical electromagnetic code”) software package for antenna modeling. See [6] for details on steering vector normalization and how to use NEC to complete calibration.

### 3.1.2 Limitations of the model

The model of direction-of-arrival has a single angular parameter  $\theta$ . Thus, in estimating the signal’s source, we are inherently limited to a two-dimensional position space. A spherical coordinate  $(r, \theta, \varphi)$  specifies a point in  $\mathbb{R}^3$  as follows:  $r$  is the distance to the origin,  $\theta$  is an angle in the  $xy$ -plane orthogonal to the  $z$ -axis, and  $\varphi$  is an angle in the plane defined by  $\theta$  and the  $z$ -axis. Thus, a bearing from receiver to transmitter in space can be described by a pair of angles  $(\theta, \varphi)$ . Our model ignores the elevation parameter  $\varphi$  completely; hence, if the signal recorded for steering vector  $\mathbf{g}(\theta)$  were significantly different for various values of  $\varphi$ , our model wouldn’t work at all in practice.

DOA models with two angular parameters have been proposed [10], but this approach is made difficult by the requirement to collect steering vectors in two angular dimensions for each site. In the one-dimensional case, we need only calibrate points on the edge of a circle encompassing the antenna array; in the two-dimensional case, we would need to calibrate points on the surface of a sphere. Moreover, the antenna was not designed to account for an elevation parameter [6]. We believe it is reasonable to assume an effective range of  $\varphi$  values, e.g. plus or minus  $45^\circ$  of the antenna’s horizon, for which elevation negligibly affects the signal; however, this point needs to be justified empirically. We stress that this effective range would have implications for the optimal antenna placement in a particular study area.

Another issue inherent to all direction-of-arrival systems is the measurement error induced on the bearing estimate when the target is far away. Suppose the steering vectors are sampled at whole-degree intervals. The transmitter’s true bearing will usually fall between two whole-degree bearings; at a distance of one kilometer from the transmitter, the width of the wedge between bearings is  $2 \cdot \sin(\pi/360) \approx 17$  meters, an unacceptable amount of error for some studies. This is another issue that should be accounted for when deciding where to place receivers. Of course, this affect can be mitigated by higher resolution calibration.

## 3.2 Bearing space

Direction-of-arrival is a well-studied subject, and as such there are a number of methods in the literature that can be adapted to our signal model and antenna pattern; we indicate a few of these and describe how they can be applied to our observations. All of these methods optimize a bearing parameter  $\theta \in [0, 2\pi]$  with

respect to an objective function called the *bearing spectrum* that depends on the observation. For example, the maximum likelihood estimator (MLE) for our model is the following:

$$\begin{aligned}\hat{\theta}_{mle} &= \operatorname{argmax}_{\theta} \ln f(\mathbf{v}, \rho, \Sigma | \theta) \\ &= \operatorname{argmax}_{\theta} (-\ln \pi^n - \ln(\det R) - \mathbf{v}^H R^{-1} \mathbf{v}) \\ &= \operatorname{argmin}_{\theta} (\ln(\det R) + \mathbf{v}^H R^{-1} \mathbf{v})\end{aligned}\tag{9}$$

The bearing spectrum is simply the log-likelihood of the probability density function in our model. Bartlett's estimator [9] is an alternative algorithm with low computational overhead, making it suitable for realtime tracking applications:

$$\hat{\theta}_b = \operatorname{argmax}_{\theta} (\mathbf{g}(\theta)^H \mathbf{v} \mathbf{v}^H \mathbf{g}(\theta))\tag{10}$$

There are yet other algorithms for direction finding that could be applied to our observations. A well-known class of noise- and signal-subspace optimization algorithms known as MUSIC may also be applied in our model [9].

We stress that these functions, while defined as continuous circular distributions, have a discrete domain in practice; this is inherent in the fact that antennas must be calibrated for known bearings. Let  $j$  denote the bearing spectrum of the observation  $(\mathbf{v}, \rho, \Sigma)$ . In what follows, we refer to  $j$  interchangeably with the set  $\{(\theta, j(\theta))\}_{\theta \in D}$  where  $D$  is a discrete subset of bearings to the receiver corresponding to calibrated steering vectors.

### 3.3 Position space

We now extend the foregoing discussion to estimate the position of the transmitter, given the bearing spectrums of a number of receivers. Consider a set of receiver sites with labels  $1, 2, \dots, k$ , positions  $(x_1, y_1), (x_2, y_2) \dots (x_k, y_k) \in \mathbb{R}^2$ , and steering vectors  $\mathbf{g}_1(\cdot), \mathbf{g}_2(\cdot) \dots \mathbf{g}_k(\cdot)$ . Suppose all sites are tuned to the same frequency on which a transmitter is emitting a signal. At some moment the sites record the set of observations  $(\mathbf{v}_1, \rho_1, \Sigma_1), (\mathbf{v}_2, \rho_2, \Sigma_2) \dots (\mathbf{v}_k, \rho_k, \Sigma_k)$ . Let  $S_i = (\mathbf{v}_i, \rho_i, \Sigma_i)$ . By  $j_i$  denote the bearing spectrum for site  $i$ .

For an arbitrary direction finder,  $j_i(\theta)$  indicates a measurement of “likelihood” of bearing  $\theta$  from site  $i$ . One may think of the sum  $j_1(\beta_i(x, y)) + j_2(\beta_2(x, y)) + \dots + j_k(\beta_k(x, y))$  as a measurement of angular agreement for transmitter position  $(x, y)$  with respect to the various observations and “likelihood” metric of  $j$ ; the point in  $\mathbb{R}^2$  that maximizes (resp. minimizes) the angular agreement of our observation may be a good estimate for the signal’s source. We can use this intuitive idea to construct an objective function  $J : \mathbb{R}^2 \rightarrow \mathbb{R}$  for numerical position estimation algorithms based on the bearing spectrum from multiple observation points.

Before defining this function, we must attend to a subtle point of practical importance. In analyzing the statistical significance of our estimates, we will require that  $J$  defines a differentiable surface in  $\mathbb{R}^2$ , and thus its domain must be continuous. Since the steering vectors  $\mathbf{g}_i(\theta)$  are not defined for all  $\theta \in [0, 2\pi]$ , we must interpolate for continuous values in the bearing spectrum so that  $j_i(\beta_i(x, y))$  is defined for all  $i$  and candidate positions  $(x, y) \in \mathbb{R}^2$ . Simple linear interpolation does not suffice, as it doesn’t yield a differentiable surface. This follows from the observation that the boundaries between segments in the bearing spectrum aren’t differentiable in general. In practice, we have observed that linear interpolation results in estimates that fall along whole-degree bearings to sites, since we recorded signals at whole degree bearings for calibration and these correspond to local optima in the interpolated spectrum.

We have found that spline interpolation [19] is a method yielding a differentiable objective function that works well in practice. Let  $\Phi[j_i]$  denote a one-dimensional spline interpolation of bearing spectrum  $j_i$ . That is,  $\Phi[j_i]$  is a spline fit to the set of  $(\theta, j_i(\theta))$  pairs for each known  $\theta$ . We may now define our objective function for position estimation:

$$J(x, y) = \sum_{i=1}^k \Phi[j_i](\beta_i(x, y))\tag{11}$$

We call  $J$  evaluated at  $(x, y)$  the  $J$ -value of that point. In section 3.3.2 we describe an algorithm for optimizing over  $J$  to obtain an estimate  $(\hat{x}, \hat{y})$  of the transmitter's location. In section 3.4 we derive the covariance of the estimate  $(\hat{x}, \hat{y})$  and describe how this could be used to generate a confidence region.

### 3.3.1 Maximum likelihood estimation

In order to motivate this approach, we consider the construction of the maximum likelihood estimator for the signal's source with respect to our model. We consider the joint probability distribution on the set  $\{S_1, S_2 \dots S_k\}$  given  $(x, y)$  the source of the signal. Recall our model of the received signal,  $\mathbf{v} = T\mathbf{g}(\theta) + \mathbf{n}$ ; in the position setting, we have  $\mathbf{v}_i = T_i \mathbf{g}_i(\beta_i(x, y)) + \mathbf{n}_i$  for each site  $i$ . Let us assume for the moment that the transmission coefficients (resp. the noise vectors) are identically and independently distributed: in particular, that

$$T_1 \dots T_k \sim \mathcal{N}(0, \sigma_T^2) \text{ and } \mathbf{n}_1 \dots \mathbf{n}_k \sim \mathcal{N}(0, \sigma_n^2 \mathbf{I}). \quad (12)$$

This implies that the observations are independent and identically distributed. Hence, if the maximum likelihood estimator (equation 9) is used for the bearing spectrum, then  $J$  is the maximum likelihood estimator for the signal source in our model. Recall the probability density function  $f(\mathbf{v}_i, \rho_i, \Sigma_i | \theta)$  (equation 6) for the observation  $S_i$  from site  $i$  given direction-of-arrival  $\theta$ . Then

$$J_{mle}(x, y) = \hat{l}(x, y; S_1, S_2 \dots S_k) = \sum_{i=1}^k \Phi[\ln f](\mathbf{v}_i, \rho_i, \Sigma_i | \beta_i(x, y))$$

is a well-defined, differentiable function of  $\mathbb{R}^2$ , and the ML estimate of  $(x, y)$  given  $\{S_1, S_2 \dots S_k\}$  is

$$(\hat{x}, \hat{y}) = \operatorname{argmax}_{x, y} J_{mle}(x, y). \quad (13)$$

We remark that the statement of (12) amounts to the assumption that the signal-to-noise ratio is the same for all sites. A well-known phenomenon in physics called the “inverse-square law” asserts that the strength of the transmitter's signal is inversely proportional to the squared distance between the transmitter and the receiver; hence, the signal-to-noise ratio is only constant if the receivers are equidistant to the transmitter. As a result, it is clearly *not* reasonable to assume that the transmission coefficients are identically distributed in general. This presents a difficulty for deriving the maximum likelihood estimate of position in our signal model. One possibility would be to model the transmission coefficient as a deterministic function of the transmitter power and distance to receivers. We consider this approach for evaluating the performance of our system in section 4. In spite of this difficulty, position estimators derived from direction finders such as the MLE in our model or Bartlett's estimator appear to perform well in practice. We consider the statistical properties of these algorithms in section 3.4.

### 3.3.2 An iterative optimization algorithm

In general a closed-form for the optimal  $J$ -value cannot be obtained. Nevertheless, there are many well-known algorithms for finding a globally optimal solution for our search space numerically. Because we wish our system to be capable of bulk processing signals into positions for many transmitters simultaneously, we need a fast algorithm that runs in time independent of the objective function. We propose the following iterative algorithm (figure 3). Starting at some coarse-grained scale, generate a grid of points around the initial guess (e.g. centroid of receiver locations) and compute their  $J$ -values. The optimal value is chosen as the new guess and a grid of finer scale is generated around it. This process is repeated until the desired resolution is reached. Note that, like most multi-dimensional optimization strategies, our solution is not guaranteed to converge to the optimum; however, we found that parameters that work well in practice, at least for our system, are  $\Delta = 5$ ,  $s = 10$ ,  $m = 3$ , and  $n = -1$ .

```

def PosEST( $(x_1, y_1) \dots (x_k, y_k), J, s, m, n, \Delta$ ) :
     $(\hat{x}, \hat{y}) \leftarrow \text{CENTROID}(x_1, y_1) \dots (x_k, y_k)$ 
    for  $\delta \in \{\Delta^m, \Delta^{m-1} \dots \Delta^n\}$  do
         $P \leftarrow \emptyset$ 
        for  $i \in \{0, 1 \dots 2s\}, j \in \{0, 1 \dots 2s\}$  do
             $P \leftarrow P \cup (\hat{x} - \delta(s-i), \hat{y} - \delta(s-j))$ 
         $(\hat{x}, \hat{y}) \leftarrow \text{opt}_{(x,y) \in P} J(x, y)$ 
    return  $(\hat{x}, \hat{y})$ 

```

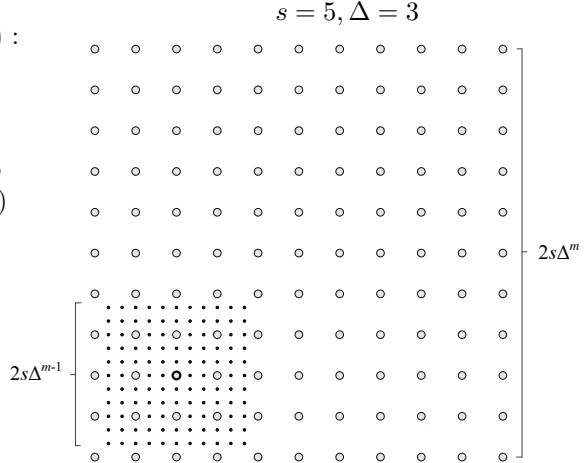


Figure 3: Iterative algorithm for estimating the source of a signal given  $J$ . Generate a grid of points centered around  $(\hat{x}, \hat{y})$ , choose the most likely as the next center. Reduce the scale and repeat.  $\Delta$ —the scaling factor in meters;  $s$ —the span of the search space, i.e.  $1/2$  the number of points spanning the side of the grid;  $m$ —the starting resolution for the search, e.g. the grid points are spaced  $\Delta^m$  meters apart;  $n$ —the target resolution for the search.  $\text{opt}$  is either  $\text{argmin}$  or  $\text{argmax}$ , depending on the bearing spectrum used. Finally, we assert that  $m > n$  and  $s \geq \Delta$ .

### 3.4 Measuring uncertainty

In this section, we generalize our solution to account for problems that arise in real time tracking scenarios. We then derive the covariance and confidence regions with respect to the new objective function.

Thus far, we have considered an instantaneous observation of the signal from  $k$  sites for position estimation, but there are a number of reasons why this scenario is not quite realistic. Recall that we think of the transmitter's modulation concretely as a periodic pulse on some frequency known to the receiver. In fact, this is the nominal mode of operation of the QRAAT system. At the core of our software defined radio is a pulse detector, a software designed to trigger a recording of the antenna channels (and a sample of the background noise) when a pulse arrives. A false positive in the triggering mechanism occurs as a result of anomalies in the noise, such as a sudden spike above the noise floor; a false negative occurs when the noise floor is too high for the pulse's signal to be represented in the spectrum, for example, when the target is far away from the receiver. Even in continuous modulation schemes there is a need to discriminate the true signal from everything else; therefore, we must account for data rates that vary between receivers.

We extend the problem to estimate the source of the signal over a given time window by aggregating the observations into an objective function, assuming the position of the transmitter doesn't change within the window. Fix a bearing spectrum function  $j$ , a time interval  $w = (t_{start}, t_{end})$ , and let  $m_i$  denote the number of pulses recorded at site  $i$  within the window. Let  $S_{i,t} = (\mathbf{v}_{i,t}, \rho_{i,t}, \Sigma_{i,t})$  denote a the  $t$ -th observation of site  $i$  where  $1 \leq t \leq m_i$ . Let  $j_{i,t}$  denote the bearing spectrum of  $S_{i,t}$ . The objective function for the position of the transmitter over time window  $w$  is:

$$J(x, y) = \sum_{i=1}^k \Phi \left[ \frac{1}{m_i} \sum_{t=1}^{m_i} j_{i,t} \right] (\beta_i(x, y)) \quad (14)$$

Next, we consider the asymptotic covariance of  $(\hat{x}, \hat{y}) = \text{opt}_{x,y} J(x, y)$  assuming that it is an unbiased estimate of the true parameter.

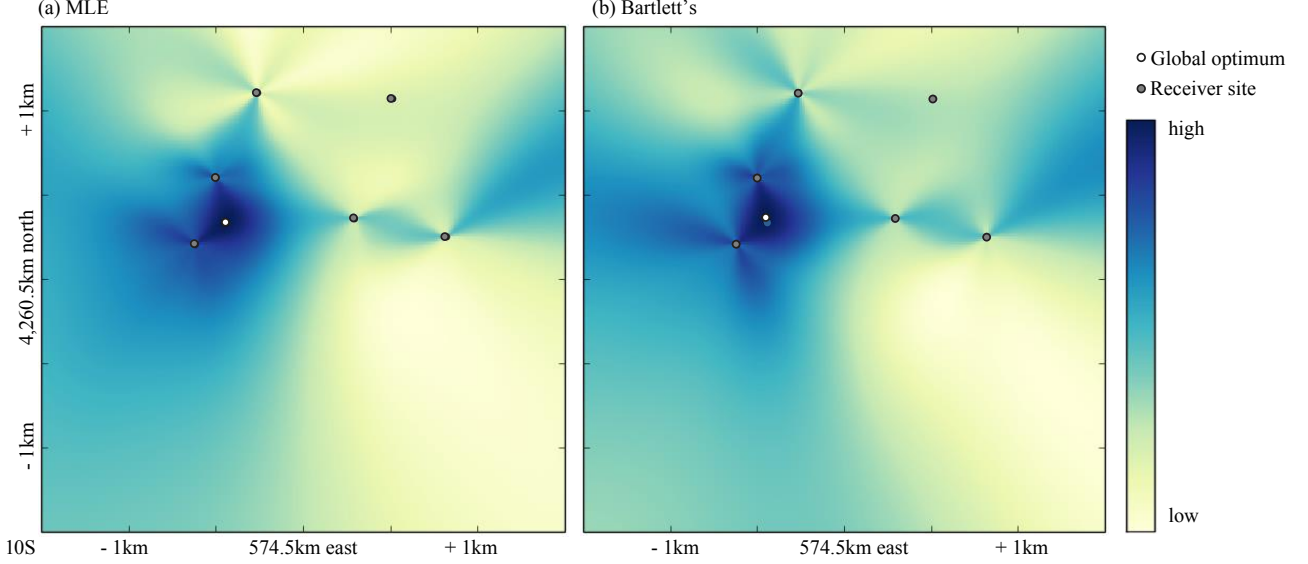


Figure 4: Illustration of the search space induced by (a) the maximum likelihood estimator for the model (eq. 9) and (b) Bartlett’s estimator (eq. 10). A woodrat was tagged with a transmitter and let loose in a study area at the Quail Ridge natural reserve and the data were collected at radio receivers deployed across reserve. The estimators were computed from 21 total samples recorded at 5 sites over a 30 second interval. The plots show the  $J$ -value of positions on a  $3 \times 3$  km grid spanning much of the reserve. Dark regions indicate high likelihood and light regions low likelihood. A translucent marker is shown in (b) to indicate the location of the ML estimate.

### 3.4.1 Asymptotic covariance of estimates

We outline the approach of [13, §2.4.2] for deriving the asymptotic covariance for the quantity  $\hat{\mathbf{x}} = \text{opt}_{\mathbf{x}} J(\mathbf{x})$ , where  $J : \mathbb{R}^2 \rightarrow \mathbb{R}$  is a continuous function. Let  $\mathbf{x}^* \in \mathbb{R}^2$  denote the true location of the transmitter. We shall assume that the estimate  $\hat{\mathbf{x}}$  is unbiased and normally distributed with mean  $\mathbf{x}^*$ . By definition, the covariance matrix is

$$\begin{aligned} C &= E[(\hat{\mathbf{x}} - E[\hat{\mathbf{x}}])(\hat{\mathbf{x}} - E[\hat{\mathbf{x}}])^T] \\ &= E[(\hat{\mathbf{x}} - \mathbf{x}^*)(\hat{\mathbf{x}} - \mathbf{x}^*)^T] \end{aligned}$$

since  $E[\hat{\mathbf{x}}] = \mathbf{x}^*$  if the estimate is unbiased. Because  $\hat{\mathbf{x}}$  corresponds to an optimum of  $J$ , we have that

$$\frac{\partial J(\mathbf{x})}{\partial \mathbf{x}} \Big|_{\mathbf{x}=\hat{\mathbf{x}}} = 0. \quad (15)$$

Assuming  $\hat{\mathbf{x}}$  is reasonably close to the true position, we can use Taylor’s series expansion around  $\mathbf{x}^*$  [14] to obtain the following result:

$$\begin{aligned} 0 &= \frac{\partial J(\mathbf{x})}{\partial \mathbf{x}} \Big|_{\mathbf{x}=\hat{\mathbf{x}}} \approx \frac{\partial J(\mathbf{x})}{\partial \mathbf{x}} \Big|_{\mathbf{x}=\mathbf{x}^*} + \frac{\partial^2 J(\mathbf{x})}{\partial \mathbf{x} \partial \mathbf{x}^T} \Big|_{\mathbf{x}=\mathbf{x}^*} (\hat{\mathbf{x}} - \mathbf{x}^*) \\ \implies -\nabla(J(\mathbf{x}^*)) &\approx H(J(\mathbf{x}^*))(\hat{\mathbf{x}} - \mathbf{x}^*) \\ \implies (\hat{\mathbf{x}} - \mathbf{x}^*) &\approx -H(J(\mathbf{x}^*))^{-1}\nabla(J(\mathbf{x}^*)) \end{aligned} \quad (16)$$

where  $\nabla(J(\mathbf{x}^*))$  and  $H(J(\mathbf{x}^*))$  are the gradient vector and Hessian matrix of  $J$  respectively, evaluated at the true position. Let  $A = H(J(\mathbf{x}^*))$  and  $\mathbf{b} = \nabla(J(\mathbf{x}^*))$  so that  $(\hat{\mathbf{x}} - \mathbf{x}^*) \approx -A^{-1}\mathbf{b}$ . This implies that

$$\begin{aligned} C &\approx E[(-A^{-1}\mathbf{b})(-A^{-1}\mathbf{b})^T] \\ &= E[A^{-1}\mathbf{b}\mathbf{b}^T(A^{-1})^T] \\ &= E[A^{-1}\mathbf{b}\mathbf{b}^T(A^T)^{-1}]. \end{aligned} \quad (17)$$

Since the Hessian is the same as its transpose, we have  $C \approx E[A^{-1}bb^T A^{-1}]$ . If the second-order derivatives of the Hessian are smooth enough [15], then  $A \approx E[A]$ . Hence,

$$\begin{aligned} C &\approx E[E[A]^{-1}bb^T E[A]^{-1}] \\ &= E[A]^{-1} E[bb^T] E[A]^{-1} \\ &= E[H(J(\mathbf{x}^*))]^{-1} E[\nabla(J(\mathbf{x}^*)) \nabla(J(\mathbf{x}^*))^T] E[H(J(\mathbf{x}^*))]^{-1}. \end{aligned} \quad (18)$$

The expected values in this expression are not known in general, but we can estimate them by taking the sample mean. Suppose for the moment that each of the sites recorded exactly  $m$  pulses. Let  $J_t(\mathbf{x})$  denote the objective function constructed from all sites and the  $t$ -th pulse where  $1 \leq t \leq m$ . We obtain the following estimate of the covariance of  $\hat{\mathbf{x}}$ :

$$\begin{aligned} C &\approx \left[ \frac{1}{m} \sum_{t=1}^m H(J_t(\mathbf{x}^*)) \right]^{-1} \cdot \left[ \frac{1}{m} \sum_{t=1}^m \nabla(J_t(\mathbf{x}^*)) \nabla(J_t(\mathbf{x}^*))^T \right] \cdot \left[ \frac{1}{m} \sum_{t=1}^m H(J_t(\mathbf{x}^*)) \right]^{-1} \\ &= H\left[\frac{1}{m} \sum_{t=1}^m J_t(\mathbf{x}^*)\right]^{-1} \cdot \left[ \frac{1}{m} \sum_{t=1}^m \nabla(J_t(\mathbf{x}^*)) \nabla(J_t(\mathbf{x}^*))^T \right] \cdot H\left[\frac{1}{m} \sum_{t=1}^m J_t(\mathbf{x}^*)\right]^{-1} \\ &= H(J(\mathbf{x}^*))^{-1} \cdot \left[ \frac{1}{m} \sum_{t=1}^m \nabla(J_t(\mathbf{x}^*)) \nabla(J_t(\mathbf{x}^*))^T \right] \cdot H(J(\mathbf{x}^*))^{-1} \end{aligned} \quad (19)$$

where

$$H(J(\mathbf{x}^*)) = \begin{bmatrix} \frac{\partial^2}{\partial x^2} J(\mathbf{x}^*) & \frac{\partial^2}{\partial x \partial y} J(\mathbf{x}^*) \\ \frac{\partial^2}{\partial y \partial x} J(\mathbf{x}^*) & \frac{\partial^2}{\partial y^2} J(\mathbf{x}^*) \end{bmatrix} \text{ and } \nabla(J_t(\mathbf{x}^*)) = \begin{bmatrix} \frac{\partial}{\partial x} J_t(\mathbf{x}^*) & \frac{\partial}{\partial y} J_t(\mathbf{x}^*) \end{bmatrix}^T. \quad (20)$$

A few remarks about this expression are in order. First, the objective function  $J$  must be constructed as in equation 14 so that its first- and second-order derivatives exist over its domain. This is assured by interpolating the bearing spectra with a spline. The Hessian and gradient can then be evaluated at  $\mathbf{x}^*$  numerically. Second, we assumed critically that  $\hat{\mathbf{x}} = \text{opt}_{\mathbf{x}} J(\mathbf{x})$  is an unbiased, normally distributed estimate of  $\mathbf{x}^*$ . We justify this assumption for Bartlett's estimator (10) using simulation in section 4. Third, we required that  $\hat{\mathbf{x}}$  and  $\mathbf{x}^*$  are “sufficiently” close to each other; again, we will quantify this condition via simulation.

Finally, it should be emphasized that the covariance is only explicitly known when the true position is known. We introduce a bootstrapping method in section 3.4.3 for measuring the performance of individual position estimates where the true position is unknown.

### 3.4.2 Confidence of estimates

We proceed with the following definition of confidence region [12, §9.7]. Let  $C$  denote the covariance matrix of  $\hat{\mathbf{x}}$ , an estimate of the transmitter location  $\mathbf{x}^*$ . Let  $m$  be the number of samples recorded at each site. (For the asymptotic case, we will continue to assume this is the same for all sites.) Fix a significance level  $\gamma \in [0, 1]$  and let  $\chi_2^2(1 - \gamma)$  denote the quantile of order  $(1 - \gamma)$  from the chi-square distribution with two degrees of freedom, e.g.  $\chi_2^2(1 - 0.05) = 5.991$ . Let

$$Q(\mathbf{x}) = \frac{1}{2}(\hat{\mathbf{x}} - \mathbf{x})^T mC^{-1}(\hat{\mathbf{x}} - \mathbf{x}). \quad (21)$$

If the sample size is sufficiently large ( $J$  is constructed from enough pulses), then the ellipsoidal region of  $\mathbb{R}^2$  where  $Q(\mathbf{x}) < Q_\gamma = \chi_2^2(1 - \gamma)$  is called the  $(1 - \gamma)$ -confidence region of the estimate  $\hat{\mathbf{x}}$ .

One must take great care when drawing inferences from this construction, as the meaning of confidence is frequently misunderstood. In particular, we *cannot* speak directly of the probability that the region contains the true parameter, i.e.  $\Pr[Q(\mathbf{x}^*) < Q_\gamma]$ . The correct interpretation is as follows: when the experiment is repeated with the same parameter and a  $(1 - \gamma)$ -confidence region is constructed for each experiment, the constructed region corresponding to the estimate will contain the true parameter  $(100 \cdot (1 - \gamma))\%$  of the time.

The contour satisfying  $Q(\mathbf{x}) = Q_\gamma$  can be obtained from the eigenvalue decomposition of  $C$  as follows: let  $\lambda_1$  and  $\lambda_2$  be the larger and smaller eigenvalues of  $C$ ,  $\mathbf{v}_1 = (u, v)$  the eigenvector corresponding to  $\lambda_1$ , and  $\alpha = \arctan(v/u)$ . The ellipse is centered at  $\hat{\mathbf{x}}$  and forms an  $\alpha$ -radian angle with the  $x$ -axis. The length of the major axis is  $2\sqrt{\lambda_1 Q_\gamma}$  and the length of the minor (orthogonal) axis is  $2\sqrt{\lambda_2 Q_\gamma}$ . See figure 5 for an illustration. Note that  $C$  is the covariance of the estimate if and only if it is positive definite; if  $C$  is not positive definite, then the ellipse constructed in this way does not exist.

### 3.4.3 Bootstrap estimate of covariance

Since the covariance is known only when the true position is known, the expression of equation 19 is not useful for all intents and purposes. We present a bootstrapping approach for estimating the covariance and constructing a confidence interval. The idea of bootstrapping is to regard the sample as the population and make inferences about the population by resampling (subsampling with replacement) from the sample data.

In our case, we construct a set of objective functions from our set of observations  $\mathcal{S} = \bigcup_{i=1}^k \{S_{i,t}\}_{1 \leq t \leq m_i}$  so that each differs by at least one pulse. We optimize over each of these functions to obtain a set of estimates  $\{\hat{\mathbf{x}}_1, \dots, \hat{\mathbf{x}}_B\}$  which is partitioned into two disjoint sets of equal length. Compute the sample covariance of the first to obtain an estimate  $\bar{C}$  of the population's covariance, and compute the sample mean  $\bar{\mathbf{x}}$  of the second to estimate the population's mean. Let  $\bar{m}$  be the average number of pulses per site. Next, compute the Mahalanobis distance of each element  $\hat{\mathbf{x}}_i$  in the second set. That is, let

$$w_i = \frac{1}{2}(\hat{\mathbf{x}}_i - \bar{\mathbf{x}})^T \bar{m} \bar{C}^{-1} (\hat{\mathbf{x}}_i - \bar{\mathbf{x}}) \quad (22)$$

for each  $\hat{\mathbf{x}}_i$ . To obtain a 95%-confidence region, we choose the element  $w_{0.95} \in \{w_i\}_{1 \leq i \leq B/2}$  such that the Mahalanobis distances of 95% of the elements in the set are less than  $w_{0.95}$ . Finally, the estimated confidence region is given by

$$(\hat{\mathbf{x}} - \mathbf{x})^T \bar{C}^{-1} (\hat{\mathbf{x}} - \mathbf{x}) \leq w_{0.95}. \quad (23)$$

As in the asymptotic case, this can be obtained explicitly from the eigenvalue decomposition of the covariance. The length of the major axis is  $2\sqrt{\lambda_1 w_{0.95}}$  and the length of the minor axis is  $2\sqrt{\lambda_2 w_{0.95}}$ .

There are several ways one can imagine resampling over  $\mathcal{S}$ . Intuitively, we expect the uncertainty of our estimates to be inversely proportional to the number of samples used in the estimation; hence, the resampling method should “scale” with the overall number of samples. The simplest approach would be to aggregate the data for each of the  $k$  sites and construct an objective function from each pair of the  $k$  bearing spectra, since only two bearings are required to obtain a position. This yields  $k(k - 1)/2$  possible resamples; however, we expect to have data from 2-5 sites, so this method is usually insufficient. A more complex method overcoming this deficiency is as follows. For each site  $i$ , aggregate the bearing spectra of all combinations of pulses of length  $m_i - 1$  differing by at least one pulse. There are  $m_i$  such combinations. More formally, let  $T_1, \dots, T_{m_i} \subset \{1, 2, \dots, m_i\}$  such that  $|T_a| = m_i - 1$  and  $T_a \neq T_b$  for all  $1 \leq a < b \leq m_i$ .

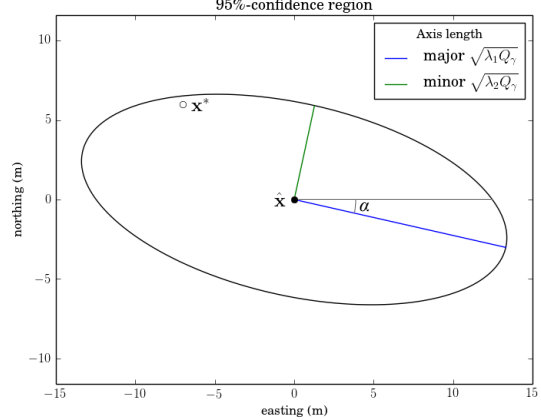


Figure 5: Confidence region from asymptotic covariance.

Let

$$j_i^{T_a}(\mathbf{x}) = \frac{1}{m_i - 1} \sum_{t \in T_a} j_{i,t}(\beta_i(\mathbf{x})). \quad (24)$$

Finally, we construct an objective function from each element in the cross product

$$\mathcal{S}' = \{j_1^{T_a}(\mathbf{x})\}_{1 \leq a \leq m_1} \times \cdots \times \{j_k^{T_a}(\mathbf{x})\}_{1 \leq a \leq m_k} \quad (25)$$

and obtain a position estimate for each. This gives us our set of positions for applying the bootstrap method above. Note that there are  $|\mathcal{S}'| = \prod_{i=1}^k m_i$  possible resamples for this method. Since this set can grow very large, we randomly sample from  $\mathcal{S}'$  some fixed number of times in practice.

## 4 Simulation

In this section, we address the assumptions made in the foregoing and evaluate the performance of the techniques indicated. We are broadly interested in two fundamental questions: first, what is performance of our position estimates under various *bad* conditions? The distribution of our estimates is influenced by a number of factors:

- *Background noise.* Our observations are recordings of radio signals so they are bound to be impacted by background radiation. Moreover, the radio receivers themselves induce a certain amount of noise on the signal. How does the background noise impact our estimates?
- *Sample size.* Intuitively, one would expect the precision of our system to improve with the number of recorded signals; on the other hand, moving targets can also induce error since we assume a fixed true position parameter in our method. The optimal sample size will likely depend on the target species and how fast it moves.
- *Distance.* As the transmitter moves away from the sites, we expect to see more error in our position estimates, since the signal degrades as a function of distance.
- *Angle.* Suppose we have two sites with which to localize a transmitter's signal. If the transmitter falls somewhere on the line formed by the two sites (the so-called *baseline*), it is impossible to localize the target with our approach. A natural question is whether or not the error on the estimator increases as the angle of intersection of the bearings to sites approaches the baseline.

There are other factors that are harder to capture. Typically there are physical features of the environment that affect the signal, and since we assume in our model that the transmitters and receivers are located on a two-dimensional plane, there is no way to account for topography. Another issue is varying data rates. When the transmitter is far away from the receiver, for example, the software defined radio may not detect a pulse, or it may detect a false pulse. This could be accounted for by modelling the pulse detector, a task outside the scope of the current work.

The second question, referring to the developments of asymptotic and bootstrap covariance of section 3.4: what is the performance of our measurement of *uncertainty* of position estimates? Is the performance affected by the conditions indicated above that influence the distribution of estimates?

We will answer these questions based on some concrete experiments in which we examine the distribution of estimates under various conditions. Because of its low computational overhead, we will use Bartlett's estimator (equation 10) as our bearing spectrum for computing the objective function. Section 4.2 deals with the affect of sample size and background noise on the distribution of estimates in an idealized environment. Section 4.3 extends this experiment by comparing the affect of angular- versus distance-error. In section 4.4 we will evaluate the performance of the asymptotic and bootstrap estimates of covariance. This experiment will use the locations of receivers and calibrations of the QRAAT instance deployed at the Quail Ridge Natural Reserve. Finally, section 4.5 provides a fine-grained, large-scale evaluation of the QRAAT system.

## 4.1 Experimental design

This section outlines the simulation method used in the experiments that follow. Let  $\mathbf{x}^*$  be the position of a transmitter with transmission power  $\rho$  and  $P = \{\mathbf{x}_1 \dots \mathbf{x}_k\}$  be the positions of  $k$  receivers. Recall that in our model the received signal at site  $i$  is  $\mathbf{v}_i = T_i \mathbf{g}_i(\theta) + \mathbf{n}$  where  $T_i$  is the transmission coefficient,  $\mathbf{g}_i(\theta)$  is the steering vector with respect to direction-of-arrival  $\theta$ , and  $\mathbf{n} \sim \mathcal{N}(0, \sigma_n^2 \mathbf{I})$ . There are  $m$  channels, so  $\mathbf{v}_i$  has length  $m$ . For the purposes of direction finding, we assumed that  $T_i$  is normally distributed with zero mean; as discussed in section 3.3.1, this is invalid in the position estimation setting since the signal degrades as a function of distance. According to the inverse-square law,

$$T_i^2 \propto \frac{\rho}{\|\mathbf{x}^* - \mathbf{x}_i\|^2}. \quad (26)$$

Hence, we will treat the transmission coefficient as a deterministic function of the transmission power and the distance to the receiver. We believe this captures the most important aspects of the experiment that are not related to the background noise.

To generate a set of observations  $\{S_{i,t}\}_{i=1}^k$  at time index  $t$ , we first scale the transmission power so that the transmission coefficients are realistic and comparable. Let  $\mathbf{x}_l \in P$  be the site nearest to the transmitter's position. Let  $\rho' = \rho \cdot \|\mathbf{x}^* - \mathbf{x}_l\|^2$  so that  $T_l^2 = \rho$ . (We've effectively declared that  $\rho$  is the received signal strength at receiver  $l$ .) For each site  $i$ , let

$$T_i = \sqrt{\frac{\rho'}{\|\mathbf{x}^* - \mathbf{x}_i\|^2}} \quad (27)$$

Next, for each site  $i$  we generate an additive noise vector  $\mathbf{n}_{i,t}$  parameterized by the variance  $\sigma_n^2 \in \mathbb{R}$ . Since the channels are assumed to be independent, circularly symmetric complex normal variables, we sample each element of the vector  $\mathbf{n}_{i,t}$  from a bivariate normal distribution as follows. Let

$$\begin{bmatrix} A_j \\ B_j \end{bmatrix} \sim \mathcal{N}\left(\begin{bmatrix} 0 \\ 0 \end{bmatrix}, \frac{1}{2} \begin{bmatrix} \sigma_n^2 & 0 \\ 0 & \sigma_n^2 \end{bmatrix}\right)$$

for  $1 \leq j \leq m$  and  $\mathbf{n}_{i,t} = [(A_1 + iB_1) \cdots (A_m + iB_m)]^T$ . Finally, let

$$\mathbf{v}_{i,t} = T_i \mathbf{g}_i(\beta_i(\mathbf{x}^*)) + \mathbf{n}_{i,t}, \quad \rho_{i,t} = T_i^2, \quad \Sigma_{i,t} = \sigma_n^2 \mathbf{I}. \quad (28)$$

Note that it is necessary in practice to interpolate for missing bearings in the steering vectors. The real and imaginary components can be handled separately. Generating a tuple  $S_{i,t} = (\mathbf{v}_{i,t}, \rho_{i,t}, \Sigma_{i,t})$  for each site  $i$  and time index  $t$  yields a data set for performing position and covariance estimation. In all experiments that follow,  $\rho = 1$ .

### 4.1.1 Measurements

Let  $Q = \{\hat{\mathbf{x}}_1 \dots \hat{\mathbf{x}}_q\}$  be a set of estimates of  $\mathbf{x}^*$  corresponding to  $q$  experiments. The variance of these estimates will be quantified in two ways. One, the *root mean squared error*:

$$\text{RMSE} = \sqrt{\frac{1}{q} \sum_{i=1}^q \|\hat{\mathbf{x}}_i - \mathbf{x}^*\|^2} \quad (29)$$

Two, the distribution of the estimates is characterized by the *empirical covariance*, a  $2 \times 2$  matrix  $\bar{\mathbf{C}}$  whose  $(j, k)$ -th entry is

$$\bar{\mathbf{C}}_{j,k} = \frac{1}{q-1} \sum_{i=1}^q (\hat{\mathbf{x}}_{i,j} - \bar{\mathbf{x}}_j)(\hat{\mathbf{x}}_{i,k} - \bar{\mathbf{x}}_k) \quad (30)$$

where  $\bar{\mathbf{x}}$  is the sample mean of  $Q$ . The *empirical 95%-confidence region* can be constructed from  $\bar{C}$  following the eigenvalue decomposition procedure of section 3.4.2, except that the ellipse is centered at  $\mathbf{x}^*$  and  $\frac{m}{2}$  is factored out of equation 21. When the estimates are unbiased and normally distributed, the ellipse will contain about 95% of the estimates.

There are three salient features of confidence intervals for measuring the performance of our position and covariance estimates. Roughly speaking, *eccentricity* is the normalized ratio of the length the minor axis to the major axis:

$$\varepsilon = \sqrt{1 - \frac{a^2}{b^2}} \quad (31)$$

where  $a$  is half of the length of the minor axis and  $b$  half of the length of the major axis.  $\varepsilon = 0$  when the region is circular and tends to 1 as the ellipse elongates. Second, we will use the *area* of the ellipse ( $\pi ab$ ) to compare the estimated covariances (asymptotic and bootstrap) to the empirical covariance. Lastly, the *coverage probability* is the percentage of time that the true position falls within the estimated confidence region of an estimated position.

## 4.2 Noise versus sample size

We begin by characterizing the distribution of estimates under ideal conditions. Two fixed receivers were used in this experiment, one placed 100 meters east of the transmitter and the other 100 meters north. Idealized steering vectors derived from the antenna model [6] were used for both sites. 10,000 simulations of this experiment were run for various noise regimes ranging from  $\sigma_n^2 = 0.001$  to  $\sigma_n^2 = 0.1$  and sample sizes ranging from 1 to 10 pulses per site.

Figure 6 illustrates the empirical distribution of estimates of the experiment for a particular noise level and sample size. In all of our experiments, we found that the sample mean converged to the true position. Moreover the eccentricity of the empirical confidence ellipse is 0 under these ideal conditions; we explore how variation in angle and distance affect eccentricity in the next section.

As the sample size increases, the root mean squared error seems to tend to 0 for all noise regimes (figure 7). This justifies the assumption in the derivation of asymptotic covariance that our estimates are unbiased. The area of the empirical confidence ellipse exhibits the same trend. The results so far suggest that it is also reasonable to assume that the estimates are normally distributed; in the next section we consider variations of the receiver configuration and examine when this assumption is still valid.

## 4.3 Angle versus distance

Next we consider varying the relative distance and angle of the sites. For the distance experiment, we set up the sites as before and ran 10,000 simulations. Site 1 was then moved 10 meters to the north and another 10,000 simulations were run. This was repeated a number of times until the ratio of the distance from site 1 to the transmitter and site 0 to the transmitter was 3:1. The noise was fixed at  $\sigma_n^2 = 0.005$  and the sample

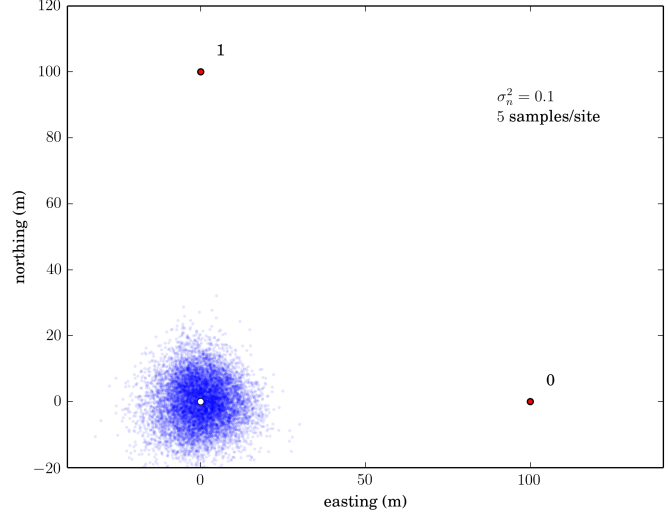


Figure 6: Distribution of estimates under ideal conditions. The estimates are shown in blue.

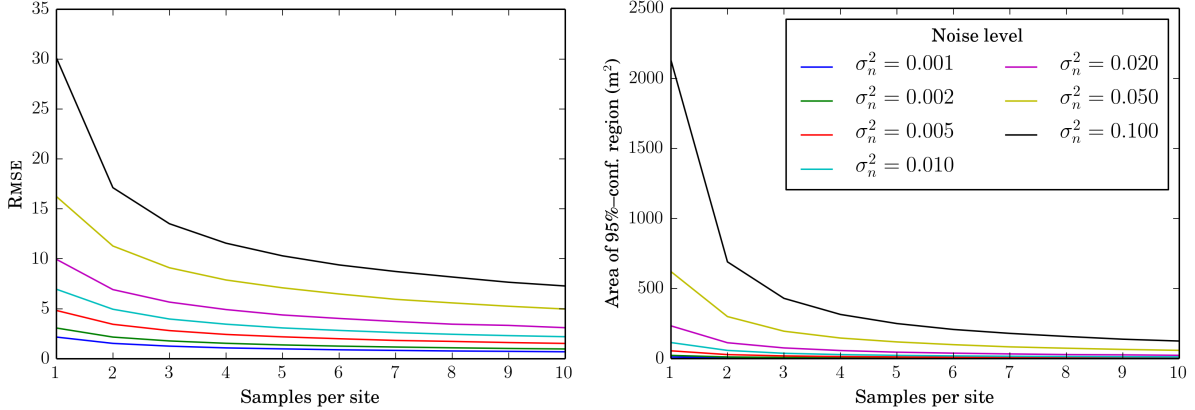


Figure 7: Position estimation error as a function of the number of samples per site and the magnitude of background noise.

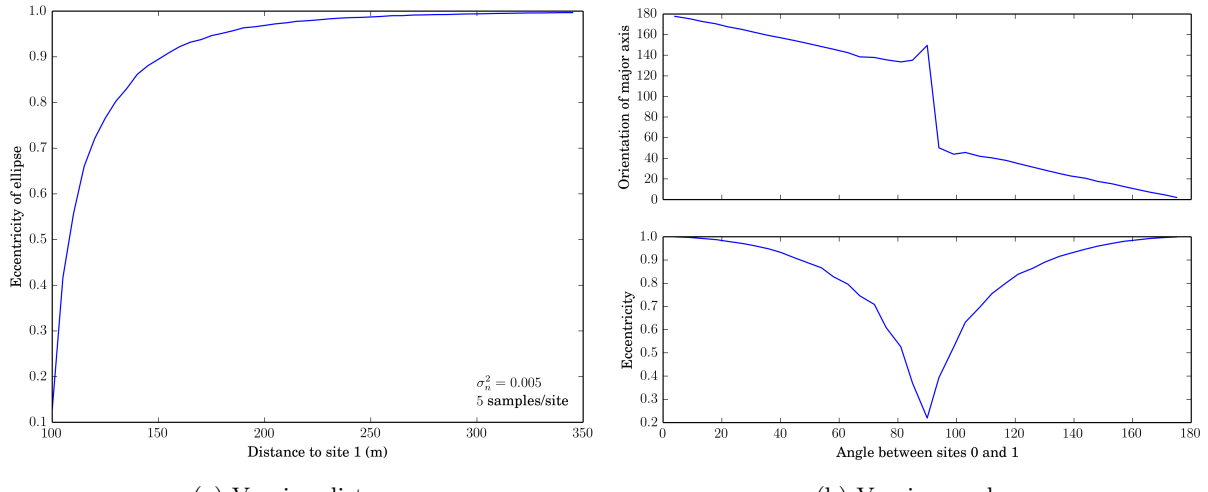


Figure 8: Eccentricity of 95%-confidence regions for varying distance and angle. The orientation of the ellipse is also shown in the case of varying angle.

size at 5 pulses per site. The eccentricity of the empirical 95%-confidence region for the various transmitter placements is shown in figure 8a.

For the angular experiment, site 0 was fixed 100 meters west of the transmitter and site 1 initially so that the distance to the transmitter was 100 meters and the angle between sites 0 and 1 (with the transmitter at the vertex) was 175.5°. (Recall that if the angle between sites 0 and 1 were 180°, the transmitter position would fall along the baseline and the most likely position would not be unique.) Site 1 was then moved so that the angle between it and site 0 varied by 4.5° increments and the distance between site 1 and the transmitter remained fixed. 10,000 simulations were run for each configuration. The eccentricity and orientation (the angle between the major axis of the ellipse and the east-west axis) of the 95%-confidence region were measured for each configuration. These values are shown in figure 8b.

As the distance increases (with fixed angle), the distribution appears to follow a normal distribution. On the other hand, as the angle of intersection approaches 0° (resp. 180°), the distribution begins to exhibit non-normal tendencies, as illustrated by figure 9c. Here the distribution is still approximately elliptical, but it tends to be more crescent-like as the transmitter gets closer to the baseline.

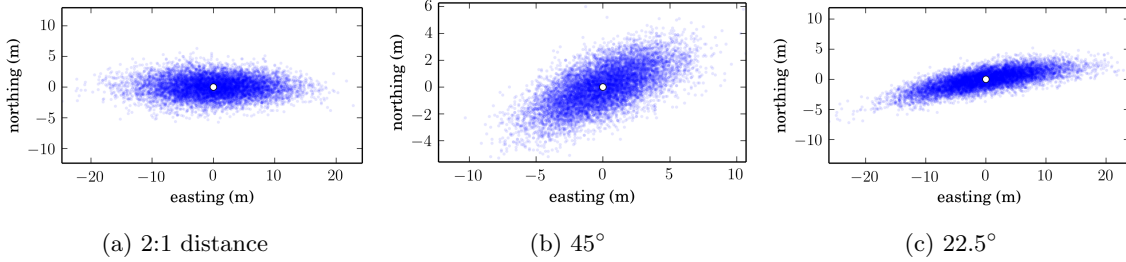


Figure 9: Illustration of estimate distributions under various conditions. (a) 100m to site 0, 200m to site 1.  $90^\circ$  between sites 0 and 1. (b) 100m to sites 0 and 1,  $45^\circ$  between sites 0 and 1. (c)  $22.5^\circ$  between sites 0 and 1.

#### 4.4 Performance of covariance estimates

In this section we evaluate the performance of our two covariance estimation methods: asymptotic covariance derived from the Taylor series expansion of the position estimator, and the bootstrap covariance estimation method for when the true position is not known. For each position estimate we derive its 95%-confidence region from both the asymptotic and bootstrap covariances and evaluate them based on their coverage probability. Our hope is that these estimates perform consistently under all of the conditions affecting the distribution of estimates outlined in the foregoing. To this end, we performed simulations for 25 grid points spaced over the Quail Ridge Natural Reserve and used the calibrations for the actual QRAAT receivers. The test grid, receivers, and empirical distributions of estimates for a particular sample size and noise regime are depicted in figure 10.

For each transmitter position, we chose the nearest 3 sites for generating signals. Although this is not quite realistic since the transmitter is unlikely to be heard at a certain distance, it allows us to test a wider variety of noisy conditions. The signal power was scaled to the distance from the center grid point to site 6. A simulation consists of generating a set of signals and estimating the position of the transmitter and the covariance of the estimate. 1,000 simulations were run for each grid point for 2, 4, 6, 8, and 10 samples and  $\sigma_n^2$  ranging from 0.001 to 0.1. For the bootstrap method, 200 resamples were performed per trial. We computed the coverage probability of the two covariance estimates for each grid point, sample size, and noise regime. The average and standard deviations of the coverage probabilities over the test grid are shown in figure 11.

The coverage probability varies wildly in the asymptotic case, suggesting that the quality of the estimate depends heavily on the geometry of the receivers. This affect may also be attributed to the “closeness” constraint indicated in section 3.4.1; in any case, we have observed that the coverage probability approves in the large sample limit, as shown in figure 12. On the other hand, the results suggest that for at least four samples per site, the coverage probability of the bootstrap estimate of covariance is roughly on target. The variance increases and the coverage probability drops as the noise level increases, indicating that the performance tends to degrade in noisier environments. However, the more samples used in the estimate, the more noise the estimate can tolerate.

#### 4.5 Evaluation of the QRAAT system

In this section we characterize the distribution of position estimates of the deployed QRAAT system. 1,000 simulations were performed for each point on a square grid spanning 2.5 kilometers with the grid points spaced 25 meters apart. For this test the samples rate was fixed at 5 per site and the noise at  $\sigma_n^2 = 0.001$ . The transmitter power was scaled so it was the same as in the previous section (4.4). All receivers within 1 kilometer of the transmitter’s location were used in the simulation.

To characterize the distribution of estimates, we compute the empirical 95%-confidence region of each grid point and plot the area, eccentricity, and orientation of the ellipse, as shown in figure 13. (In the figure, eccentricity is simply the ratio of the minor axis to the major axis, for display purposes.) The results confirm

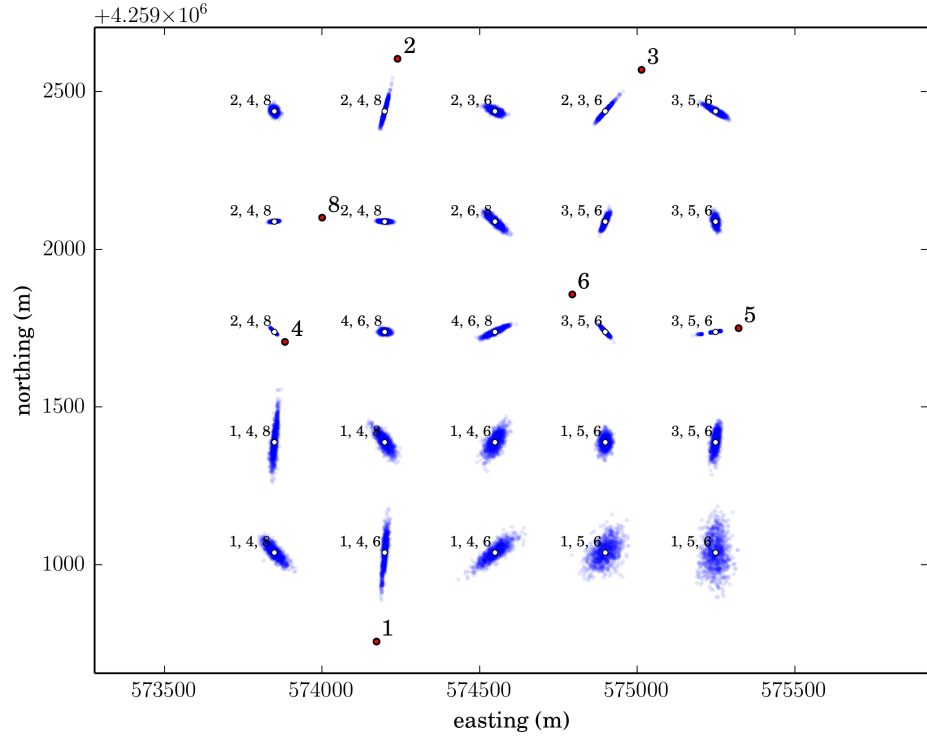


Figure 10: Empirical distributions of estimates,  $\sigma_n^2 = 0.005$  and 6 pulses per site. The locations of the receivers are shown in red. The 3 sites used in the simulations of each grid point are shown. Note the odd distribution of estimates of the position closest to site 5; this is the result of convergence errors that were fixed by changing the parameters of the search algorithm.

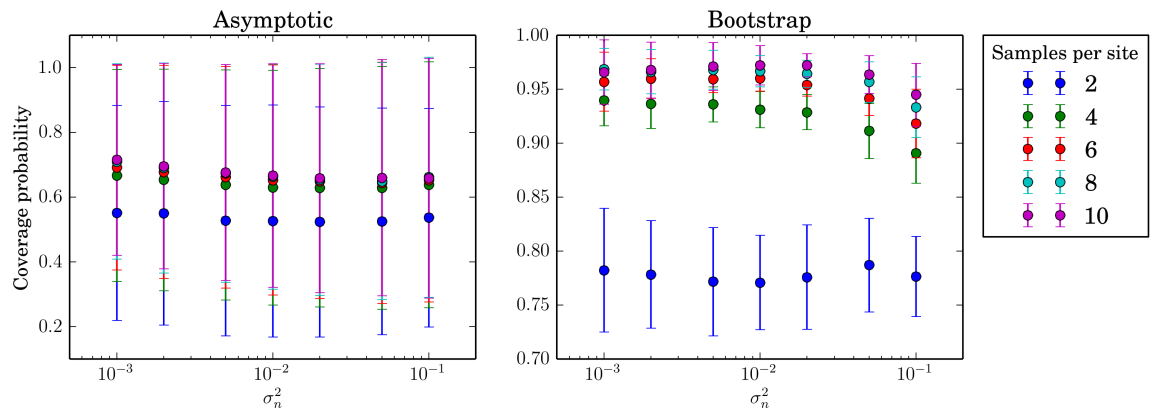


Figure 11: Coverage probability of 95%-confidence regions for asymptotic and bootstrap covariance estimates. The average and standard deviation of the coverage probabilities of the 25 test points are shown for various sample sizes and noise regimes. The  $x$ -axes are log-scaled.

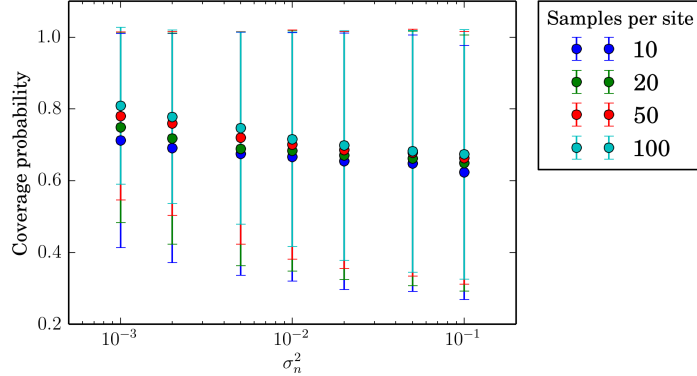


Figure 12: Coverage probability of 95% asymptotic confidence regions for large sample sizes.

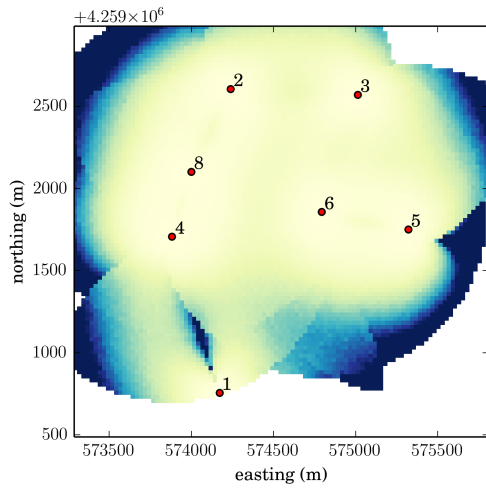
that the area of the ellipse increases as the transmitter moves away from the receivers, and that the ellipse elongates when the angle of intersections of bearings are close to the baseline. The data also reveals that the eccentricity gets worse when the transmitter is closer to one site than the others. Combining these factors yields a trade-off space in considering where to place receiver sites in a study area.

## 5 Conclusion

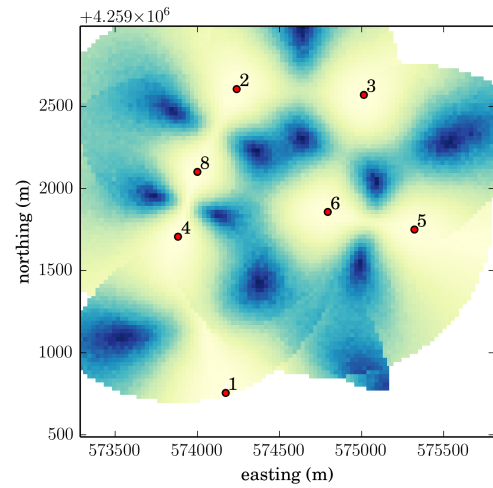
We introduce a signal model for a direction-of-arrival mode of position estimation. Given an antenna array with  $m$  channels, we model the received signal as a vector in  $\mathbb{C}^m$  with identically and independently distributed channel noise. Based on this assumption, we derive the maximum likelihood estimator for the bearing of the transmitter from the receiver with respect to a mapping from known bearings to steering vectors. The DOA method is a mature field in antenna and radio modeling; we describe a method of position estimation using an arbitrary direction finder by optimizing the angular agreement of the bearing spectra of the sites. We evaluated the performance of this method (as well as the algorithm that optimizes the objective function) with respect to Bartlett’s estimator, a well-known and computationally efficient direction finder.

A number of conditions influence the distribution of estimates; those addressed in this work are background noise on the transmission frequency (SNR), the number of samples (recordings of the signal) per receiver, the number of receivers (although not explicitly), distance to the receivers, and the angle of intersection between bearings. In order to model these affects, we modified the signal model proposed in section 3.1 so that the transmission coefficient scales as a function of distance according to the inverse-square law. Our simulations suggest that it is reasonable to assume that position estimates are unbiased, normally distributed estimates of the transmitter’s position under variable conditions; that is, the distribution behaves well when noise and sample sizes scale and the geometry of the experiment changes. The only case we found where this assumption does not hold is when the transmitter is close to the baseline between two sites. When the transmitter is directly on the baseline (the angle of intersection of the bearings is  $180^\circ$ ), the transmitter’s location cannot be discriminated, unless there is a third site sufficiently close to the transmitter to disambiguate the bearing intersection.

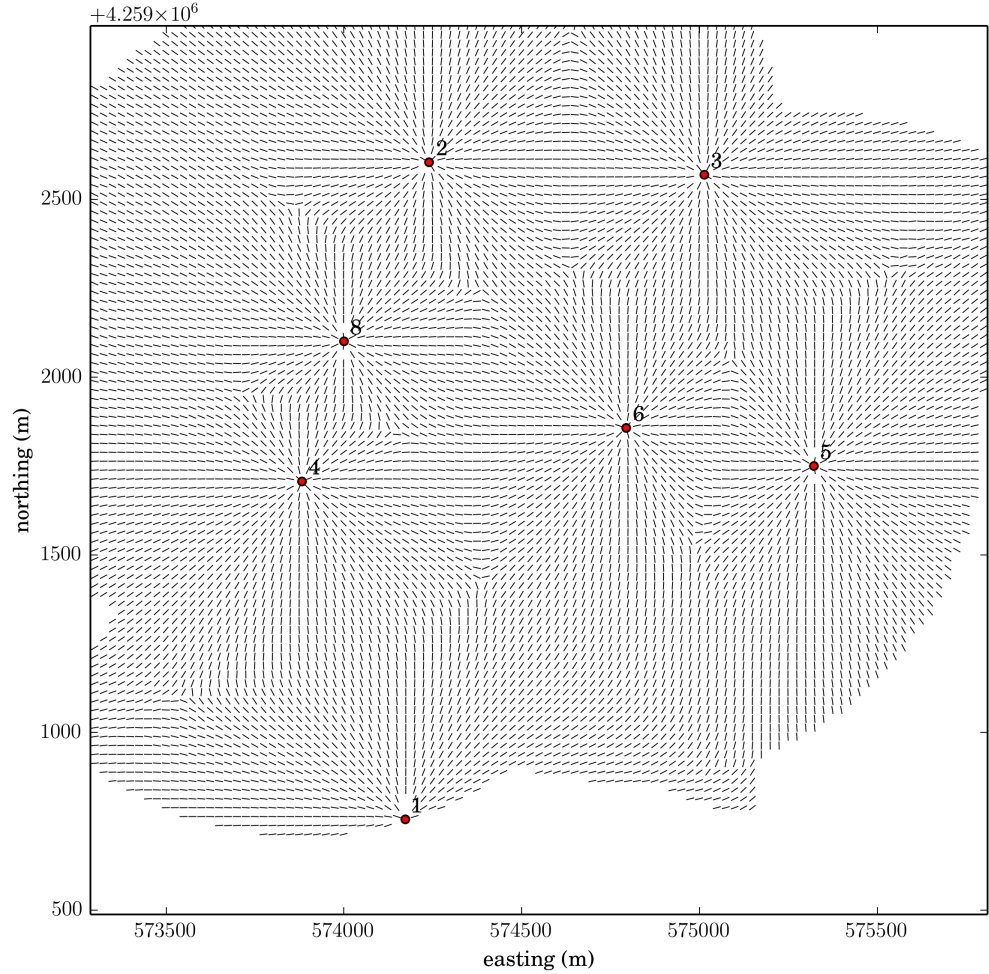
There are other factors to consider in the signal localization problem. Although we have incorporated it into our methodology, we have not evaluated the performance of our system when the data rates vary between receivers. This is a critical consideration in any practical implementation, since automated signal detection and recording is inherently susceptible to trigger errors. Another interesting extension to our model would be to represent bearings in three dimensions, allowing one to consider topography in simulations. This is a formidable challenge for a number of reasons, not the least of which would require a redesign of the antenna array since it was not designed with an elevation parameter in mind.



(a) Area. Values range from about  $10 \text{ m}^2$  (light yellow) to  $5 \text{ km}^2$  (dark blue).



(b) Ratio of minor axis to major axis. Values range from 0 (light yellow) to 1 (dark blue).



(c) Orientation of ellipse.

Figure 13: Distributions of estimates for various locations over the reserve. 5 samples per site,  $\sigma_n^2 = 0.001$ . All sites within 1 km of the transmitter were used.

Having characterized their distribution, we derived the asymptotic covariance of position estimates and constructed their  $(1 - \gamma)$ -confidence regions. This quantity depends on the differential properties of the objective function and is only known explicitly when the true position is known. The development takes advantage of a connection between the Taylor series expansion of the objective function evaluated at the true position and the definition of covariance of an unbiased, normally distributed bivariate random variable. We evaluated the performance of this estimate by computing the coverage probability (the percentage of time the true position fell within the confidence region of the estimate) for a number simulated test points representing a variety of geometric configurations. Our results suggest this is a poor estimate of covariance in the sample regime we are interested in (2-10 samples/site) and only works for large sample sizes that are unrealistic for our purposes.

In section 3.4.3 we presented a simple bootstrapping method that performs well for realistic sample sizes. Moreover, this covariance estimate does not depend on the true position making it practical for real-world systems like QRAAT. Therefore, we propose the confidence region derived from the bootstrap covariance estimate as a statistically rigorous measurement of uncertainty of our system's position estimates. The intended property of this measurement is as follows: when we estimate the position and covariance of a stationary transmitter a number of times, for 95% of these trials, the transmitter's actual location will fall within the 95%-confidence region of the estimate. Note that one may not infer for a given position estimate that there is a 95% chance the true parameter falls within the interval; this must be interpreted as a long-run rather than instantaneous probability. We stress that the distribution of the estimate changes as the target moves about, as this changes the geometry of the experiment. Besides the coverage probability, the salient features of the confidence region are the area and eccentricity of ellipse. These can be used to quantify how certain we are of a given estimate relative to other estimates.

The next iteration of this work will be to validate the model on hand of real-world data. One would replicate the experiment of section 4.4: collect a number of signal recordings (a few hours' worth) for several test points, compute position and covariance estimates, and the average coverage probability over all the test points. This should indicate that the position estimation algorithm works as advertised, whether the distribution of estimates are well-behaved (in that they are unbiased and approximately normally distributed), and that the bootstrap covariance estimate works as advertised. A point to be wary of is the function used to simulate signal degradation, as this relationship is modeled differently for different transmission environments. Lastly, in our simulations we have attempted to cover a large sample regime (three orders of magnitude) in the hopes that the observed system noise will fall within that range; if not, the simulations should be rerun with realistic SNR.

Another pending issue, discussed in section 3.1.2, is to establish an effective range in which the elevation parameter is negligible in DOA estimation for our receivers. This is a range of angles between the receiver antenna, the transmitter, and the antenna horizon; based on the antenna pattern, it seems reasonable to assume an effective range of  $\pm 45^\circ$  of the antenna horizon, but this needs to be validated experimentally.

Finally, if these experiments serve to validate our methodology, then a point of theoretical interest would be to lift the position estimator of equation 11 to a maximum likelihood estimator with respect to a realistic model of the signal. In section 3.3.1, we briefly considered adapting the MLE of the signal model for DOA (equation 9) to the position estimation setting; however, we could not assume the transmission coefficients were identically distributed, since the SNR is different for each receiver. One may first consider taking the transmission coefficient to be a deterministic function of the distance to the the true position, as we did in our simulations (section 4.1).

## Acknowledgments

This work and the QRAAT project were funded by NSF grant No. 1262654. The bootstrap covariance estimate presented in section 3.4.3 is built upon a method proposed by a group of graduate students in a statistics course taught at UC Davis (STA260, Winter 2015). I would like to thank Chun-Jui Chen and his advisor Jane-Ling Wang in particular for their invaluable contribution. Use cases, data, and insightful

comments on the practice of animal tracking were provided by Karen Mabry, Mary Brooke McEachern, Tina Wey, and several others. I would like to thank my advisor Nina Amenta for her guidance and our enlightening conversations. Thank you to Marcel for his mentorship and direction, and to Shane Wadell and Virginia Boucher for giving me a shot. Last but certainly not least, I thank Todd Borrowman for his mentorship, advice, and patience over the last few years; thanks for showing me what engineering is all about.

## References

- [1] White, Gary C. and Garrot, Robert A. 1990. *Analysis of Wildlife Radio-Tracking Data*, Academic Press Inc.
- [2] Lenth, Russell V. 1981. "On finding the source of a signal." *Technometrics*, Vol. 23, No. 2: pp. 149-154. <http://www.jstor.org/stable/pdfplus/1268030.pdf>
- [3] Anderson-Sprecher, Richard and Lenth, Russel V. 1996. "Spline estimation of paths using bearings-only tracking data." *Journal of the American Statistical Association*, Vol. 91, No. 433: pp. 276-283. <http://www.jstor.org/stable/2291405>
- [4] Zekavat, Seyed A. (Reza) et al. 2011. "Wireless positioning systems: operation, application, and comparison." In *Handbook of Position Location*, John Wiley & Sons, Inc., pp. 3-22. <http://onlinelibrary.wiley.com/doi/10.1002/9781118104750.ch2/pdf>
- [5] Gatto, Riccardo and Jammalamadaka, Sreenivasa Rao 2007. "The generalized von Mises distribution." *Statistical Methodology*, Vol. 4 (2007), pp. 341-353. <http://www.sciencedirect.com/science/article/pii/S1572312706000530>
- [6] Borrowman, Todd A. 2007. "Multichannel coherent radio receiver and direction finder for transient signals." Masters thesis, University of Illonis, Urbana-Champagne.
- [7] Pierre, J., and M. Kaveh 1991. "Experimental performance of calibration and direction-finding algorithms." International Conference on Acoustics, Speech, and Signal Processing, ICASSP-91. 1991. <http://ieeexplore.ieee.org/stamp/stamp.jsp?arnumber=150676>
- [8] Hua, Yingbo and Tapan K. Sarkar 1991. "A note on the Cramer-Rao bound for 2-D direction finding based on 2-D array." *Signal Processing, IEEE Transactions on*, Vol. 39, No. 5: pp. 1215-1218. <http://ieeexplore.ieee.org/stamp/stamp.jsp?tp=&arnumber=80958>
- [9] Dandekar, K. R., H. Ling, and G. Xu 2000. "Effect of mutual coupling on direction finding in smart antenna applications." *Electronics Letters*, Vol. 36, No. 22: pp. 1889-1891. <http://ieeexplore.ieee.org/ielx5/2220/19217/00888456.pdf?tp=&arnumber=888456&isnumber=19217>
- [10] Noohi, T., Epain, N. and Jin, C 2013. "Direction of arrival estimation for spherical microphone arrays by combination of independent component analysis and sparse recovery." ICASSP, pp. 346-349. <http://ieeexplore.ieee.org/stamp/stamp.jsp?tp=&arnumber=6637666>
- [11] Heyde, Christohper C., 1997. *Quasi-likelihood and its application: a general approach to optimal parameter estimation*, New York: Springer.
- [12] G. D. Cowan, 1998. *Statistical Data Analysis*, New York: Oxford University Press.
- [13] So, H. C. 2011. "Source Localization: Algorithms and Analysis." In *Handbook of Position Location*, John Wiley & Sons Inc., pp. 25-66. <http://onlinelibrary.wiley.com/doi/10.1002/9781118104750.ch2/pdf>
- [14] Cheung, K. W. and So, H. C. 2005. "A multidimensional scaling framework for mobile location using time-of-arrival measurements." *IEEE Trans. Signal Process.*, Vol. 53, No. 2, pp. 460-470.
- [15] MacDonald, V. H. and Schultheiss, P. M. 1969. "Optimum passive bearing estimation in a spatially incoherent noise environment." *J. Acoust. Soc Am.*, Vol. 46, No. 1: Pt. 1, pp. 37-43.

- [16] Kalman, R. E. 1960. "A New Approach to Linear Filtering and Prediction Problems." *J. Fluids Eng.*, Vol. 82, No. 1: pp. 35-45.
- [17] Horne, J. et al. 2007. "Analyzing animal movements using Brownian bridges." *Ecology*, Vol. 89, No. 9: pp. 2354-2363.
- [18] Madon, B. and Hingrat, Y. 2014. "Deciphering behavioral changes in animal movement with a 'multiple change point algorithm-classification tree' framework." *Front. Ecol. Evol.* Vol. 2, No. 30. doi: 10.3389/fevo.2014.00030
- [19] *SciPy* documentation on Spline interpolation, accessed 29 Jan 2015. <http://docs.scipy.org/doc/scipy/reference/tutorial/interpolate.html>